Phase-amplitude method applied to doubly excited states of He($^1S^e$)

John L. Bohn
The James Franck Institute and the University of Chicago, Chicago, Illinois 60637
(Received 2 June 1993)

We present a phase-amplitude (PA) procedure, which emphasizes the *evolution* of the He** wave function from the origin of the hyper-radius $R = \sqrt{r_1^2 + r_2^2}$. This method, combined with quantum-defect theory, produces an R-dependent phase shift $\pi\tau(R)$ of the ionized channel, whose variation with R illustrates explicitly its coupling with the closed resonant channels. Previous calculations (e.g., of the R-matrix type) whose dynamical information remains hidden within a core region are thus complemented and extended by displaying the R dependence of phase shifts for several low doubly excited resonances of He($^1S^e$). The large R limit yields the familiar scattering phase shift, in fair agreement with experimental data. The results illustrate the dominant role of short-range channel coupling in the formation of resonances.

PACS number(s): 32.80.Dz, 31.20.Di

I. INTRODUCTION

Two-electron atoms and ions (e.g., H^-, He, Li^+) have played a central role in the study of nonseparable problems in atomic and molecular dynamics. The Coulomb interaction between electrons—comparable in He to the nuclear field—invalidates the independent-electron quantum numbers even for the lowest doubly excited states, by generating strong correlations in the electron pair's motion. Correlations dominate this motion near the "Wannier ridge," where the electrons sit on opposite sides of the nucleus and at similar distances from it [1]. The pair proves metastable in this configuration, despite being on a saddle point of the Coulomb potential; however, at energies between the single- and double-ionization thresholds, one electron will ultimately give the other enough energy to kick it out of the atom. This ionization configuration tends toward a minimum of the Coulomb potential energy, and is thus termed a "valley" configuration. Detailed study of transitions between ridge and valley states yields insights into transfers of energy and momentum in all atomic and molecular rearrangement processes.

Many authors have approached the problem of doubly excited states from various points of view. Some, in exploring ridge states, work in configuration space near the ridge [1–4]. Others start from a basis of wave functions with both electrons starting at equal principal quantum number [5,6]. Complex-coordinate rotation methods [7], variational calculations [8,9], and the finite-element method [10] produce accurate results without displaying the mechanisms of excitation and decay explicitly. Less accurate, but very instructive, studies have utilized an adiabatic approximation in hyperspherical [11–13] or moleculelike [14] coordinates. These studies, along with group-theoretical analysis [15], have provided a semiquantitative classification of doubly excited states [12]. Adiabatic solutions have been coupled diabatically to yield Rydberg series converging to double ionization [16,17], and more general information on resonant states [18]. A recent "diabatic by sector" method has achieved further computational improvement along these lines [19]. As yet, none of these studies has shown details of the mechanisms underlying the formation and decay of ridge states. The present paper represents the first step in a comprehensive plan designed to exhibit *all* states of two-electron systems as arising from a common mechanism.

Double escape of the electron pair just above threshold was discussed first classically by Wannier [1], later semiclassically by Rau [2] and Peterkop [3]. These authors identified pairs of classical trajectories (or WKB wave fronts) converging toward and diverging from the ridge, and evaluated the probability for the pair to stay on the ridge as it escapes to infinity. The resulting threshold law for the double-ionization cross section was subsequently verified by Cvejanović and Read [20] for an electron pair escaping from a residual He^+ ion. At energies below threshold, the pair can propagate only a finite distance up the ridge before being pulled back by the nuclear attraction. In this case, the pair's motion becomes a Rydberg-like series of quasistable resonances converging to the double escape threshold [4,21], each of them eventually ejecting one electron and leaving the other in a state of principal quantum number N.

Three key aspects of this phenomenon, common to all nonseparable problems, are noted here: (1) temporary localization on ridges, i.e., at maxima or saddle points of the potential; (2) alternative localization in valley configurations of low potential; (3) a connection that allows transitions from one localization to the other. (Many intermediate configurations exist in doubly excited atoms and ions. In this discussion we focus on valley and ridge states for clarity.)

Fano and Sidky [22] have recently forged a unified wave-mechanical picture of these aspects for a simpler nonseparable situation, namely, that of a Rydberg atom in a magnetic field. In this case the valley lies *along* the magnetic field, the ridge *across* it. The wave function is expanded into spherical harmonics $Y_{lm}(\theta, \phi)$ and

their corresponding radial Coulomb functions $f_l(r)$, all but finitely many of which are excluded at fixed r by centrifugal forces. Diagonalization of the interaction in a *finite* basis results in alternative localizations in the valley and on the ridge. However, states well localized in angle at large r are not so localized at small r, owing to the smaller number of contributing harmonics. Various localizations thus have a common origin in a relatively isotropic core region at small r. This dynamics has been illustrated by the evolution of eigenfunctions of the interaction, starting from $r = 0$ and progressing toward $r \to \infty$.

This paper will take a similar view toward doubly excited states of helium, using as radial variable the hyperradius $R = \sqrt{r_1^2 + r_2^2}$. In a familar set of hyperspherical coordinates [23], the remaining five coordinates are all angles, namely, the directions $\hat{\mathbf{r}}_1$, $\hat{\mathbf{r}}_2$ of the two electrons, and a radial correlation angle α given by $\tan\alpha = r_2/r_1$, to be denoted collectively as ω. The finite range of these angular variables allows for a discrete harmonic analysis, just as in the diamagnetic problem. Spherical harmonics are replaced here by hyperspherical harmonics, with corresponding radial functions subject to generalized centrifugal barriers in R. The different harmonics will be mixed by the Coulomb interaction, just as the Y_{lm}'s of Ref. [22] were mixed by the diamagnetic potential. (As an aside, note that more general problems in atomic and molecular collision dynamics fit into the same formalism via generalized hyperspherical coordinates and harmonics [24,22].)

Calculations of He wave functions analogous to those of Ref. [22] have been carried out [25]. However, whereas a basis of Coulomb functions was appropriate to the perturbative region of Ref. [22], the analogous basis in He has so far produced intractable results. The present paper will instead take as a starting point the results of the adiabatic approximation, which treats R as an adiabatic parameter and solves the remaining problem in ω for each fixed R. This solution leads to potential curves in R which converge at large R to the thresholds for single ionization. The channels thus defined already display R-dependent correlations in their angular functions. The channel classification afforded by the adiabatic functions [12] will simplify our further analysis a great deal.

The main shortcoming of the adiabatic approximation lies in its deliberate neglect in zeroth order of hyperradial and hyperangular correlations generated by d/dR terms of the Hamiltonian. In particular, it neglects the channel couplings responsible for autoionizing transitions. These couplings will now be included to all orders by a phase-amplitude (PA) method similar to that of Ref. [22], thus admixing the adiabatic channels progressively as R increases. The correct large-R behavior of the coupled channel functions will be enforced through an analysis akin to multichannel quantum-defect theory (MQDT) [26], yielding R-dependent phase shifts in all the open channels, and thereby a picture of the evolving states. These phase shifts converge at moderate R to their asymptotic values, whose energy dependence reflects the positions and widths of the autoionizing resonances.

This paper deals only with low doubly excited states of He in order to illustrate method and results. This is the "discrete" side of the problem, where the single-ionization thresholds N are well separated in energy. The ideas developed here, however, should allow future work to ascend to the double-ionization threshold, and beyond it, making contact with the "continuum" Wannier theory.

II. THEORETICAL FRAMEWORK

A. Adiabatic approximation

We begin by reproducing the basic formulation of the hyperspherical adiabatic treatment of two-electron systems. In the hyperspherical coordinates introduced above, the Schrödinger equation in atomic units reads [11]

$$\left(-\frac{\partial^2}{\partial R^2} + \frac{\Lambda^2 + \frac{15}{4}}{R^2} - 2\frac{C(\omega)}{R} - 2E\right)\psi(R,\omega) = 0. \quad (1)$$

Here, Λ is the "grand angular momentum" operator,

$$\Lambda^2 = -\frac{1}{\sin^2\alpha\cos^2\alpha}\frac{\partial}{\partial\alpha}\left(\sin^2\alpha\cos^2\alpha\frac{\partial}{\partial\alpha}\right) + \frac{\boldsymbol{l}_1^2}{\cos^2\alpha} + \frac{\boldsymbol{l}_2^2}{\sin^2\alpha}, \quad (2)$$

and $C(\omega)$ is an effective charge, depending on the angular coordinates through

$$C(\alpha,\theta_{12}) = \frac{Z}{\sin\alpha} + \frac{Z}{\cos\alpha} - \frac{1}{(1-\sin 2\alpha\cos\theta_{12})^{1/2}}, \quad (3)$$

where $\cos\theta_{12} = \hat{\mathbf{r}}_1 \cdot \hat{\mathbf{r}}_2$ and Z is the nuclear charge (=2 in He). In (1) we have renormalized the wave function $\bar{\psi} = R^{-5/2}\psi$, so that ψ vanishes at $R = 0$.

As mentioned in the Introduction, we want to exploit the finite range of the angular variables to make a discrete harmonic analysis. An appropriate set of hyperspherical harmonics are the eigenfunctions of Λ^2,

$$\Lambda^2 u_{l_1 l_2 n_r} = \lambda(\lambda+4)u_{l_1 l_2 n_r},\ \lambda = l_1 + l_2 + 2n_r. \quad (4)$$

These harmonics, described in detail in Ref. [27], need not be reproduced here. The quantum numbers l_1 and l_2 represent angular momenta of the two electrons, and n_r (the radial correlation quantum number) counts the nodes in α. At small R, the centrifugal term of (1) dominates the Coulomb term, and the problem separates into products of R-dependent functions and of these u's. As R grows, off-diagonal Coulomb terms mix the harmonics into the two-electron wave functions.

An initial procedure for mixing these harmonics mimics the Born-Oppenheimer approximation of molecular physics. Here, R is viewed as a slowly varying coordinate relative to the angles ω. Then the $\partial/\partial R$ term of (1) is insignificant and the angular problem reduces to the eigenvalue equation [11]

$$\left(\Lambda^2+\frac{15}{4}-2RC(\omega)\right)\Phi_\mu(R;\omega)=R^2V_\mu(R)\Phi_\mu(R;\omega). \tag{5}$$

This equation organizes the problem into various adiabatic channels, labeled here by μ, each of whose angular functions $\Phi_\mu(R;\omega)$ exhibits a characteristic correlation pattern in ω. These channels form the basis of Lin's classification scheme for two-electron states [12], results of which we will reproduce as necessary in the following. Upon expanding C and Φ_μ into the harmonics (4), Eq. (5) becomes a discrete eigenvalue problem at each R, whose dimension is finite because centrifugal barriers suppress high λ's.

Radial motion, secondary in this approximation, is governed by the potential wells $V_\mu(R)$. Macek found lower states of these wells to give a good first approximation to the energies of doubly excited resonances [11]. At sufficiently large R, each channel function $\Phi_\mu(R;\omega)$ falls into a potential valley, characterized by maximum amplitude near $\alpha\sim 0$ and $\alpha\sim\pi/2$. Accordingly, the potential $V_\mu(R)$ associated with this channel approaches the ionic energy $-Z^2/2N^2$ appropriate to the escape of a single electron to infinity with zero kinetic energy. The bound states of these wells are truly bound, since their only energetically allowed escape route lies in channels converging to a lower N. By ignoring channel couplings, the adiabatic approximation fails to describe autoionization.

B. Channel mixing

To include this coupling, the adiabatic solutions themselves must be mixed as R increases. The wave function thus takes the form

$$\Psi_{\mu_0}(R,\omega)=\sum_{\mu'}\Phi_{\mu'}(R;\omega)F_{\mu'\mu_0}(R), \tag{6}$$

whose subscript μ_0 emphasizes that the adiabatic solutions are unmixed at small R, i.e., $F_{\mu\mu_0}(R)\propto\delta_{\mu\mu_0}$ for sufficiently small R. Substituting (6) into the Schrödinger equation (1) and projecting onto a particular Φ_μ produces a set of coupled equations [11]

$$-\sum_{\mu'}\left(\mathbf{I}\frac{d}{dR}+\mathbf{P}\right)^2_{\mu\mu'}F_{\mu'\mu_0}(R)=[2E-V_\mu(R)]F_{\mu\mu_0}(R), \tag{7}$$

where channel coupling originates in the operator $\mathbf{P}$, defined as

$$P_{\mu\mu'}\equiv\left\langle\Phi_\mu\middle|\frac{\partial\Phi_{\mu'}}{\partial R}\right\rangle=-P_{\mu'\mu}, \tag{8}$$

and the brackets denote integration over ω. The significance of $\mathbf{P}$ is as follows: in an adiabatic bound state μ, the electron pair's radial momentum can take it only to the outer turning point of its potential V_μ. Off-diagonal connections boost the radial momentum of the pair to another channel μ' of greater kinetic energy, via the momentum operator d/dR.

The mixing of adiabatic functions also mixes their radial functions. In particular, since the differential relations between F's are second order in R, $F_{\mu\mu_0}$ must combine two linearly independent solutions f_μ and g_μ:

$$F_{\mu\mu_0}=f_\mu(R)a_{\mu\mu_0}(R)+g_\mu(R)b_{\mu\mu_0}(R). \tag{9}$$

To simplify the boundary conditions at $R=0$, we choose all f_μ's to be regular there. The appropriate boundary condition is then $a_{\mu\mu_0}(0)\propto\delta_{\mu\mu_0}$,$b_{\mu\mu_0}(0)=0$. The radial adiabatic functions are conveniently represented through their Milne phases $\phi_\mu(R)$ [28]:

$$f_\mu=\alpha_\mu(R)\sin\phi_\mu(R),\ \alpha_\mu(R)=\left(\frac{2}{\pi\frac{d\phi}{dR}}\right)^{1/2}. \tag{10}$$

These f_μ's are energy-normalized solutions to the uncoupled radial equations in the potentials $V_\mu(R)$. The phase-amplitude form (10) defines the irregular solution as $g_\mu=\alpha_\mu\cos\phi_\mu$, a form that exhibits the mixing in (9) as a set of R-dependent phase shifts. This emphasis on channel mixing represented by a variable phase is the essence of the PA method of Zemach and Calogero [29].

Instead of integrating the coupled equations for a's and b's directly, we will integrate equations for a short-range reaction matrix, defined as in Ref. [22]:

$$K_{\mu\mu'}(R)=\sum_{\mu''}b_{\mu\mu''}\left(a^{-1}\right)_{\mu''\mu'}. \tag{11}$$

A similar K is familar from scattering theory, where it is calculated at a certain appropriate radius to represent particle interactions, or more generally channel interactions, *within* that radius. K then serves to mix the noninteracting independent-channel wave functions beyond this radius. The novelty of this method is to calculate such a K at *each* radius, thus charting the evolution of wave functions as R grows. This information is best expressed by diagonalizing K,

$$K_{\mu\mu'}=\sum_p\langle\mu|p\rangle\tan\delta_p\langle p|\mu'\rangle, \tag{12}$$

with eigenvectors $|p(R)\rangle$ characterized by a common eigenphase shift $\delta_p(R)$.

Reference [22] applies the PA method to an R-dependent potential in the diamagnetic problem. The present situation differs in that the angular basis functions Φ_μ depend parametrically on R, whereby the coupling operator $\mathbf{P}$ in Eq. (8) depends on R through the derivative d/dR. Application of the PA procedure as in Ref. [22] leads then to an asymmetric K matrix.

Babamov [30] has indicated how to avoid this difficulty by defining the "adiabatic momentum operator" ∂:

$$\partial_{\mu\mu'}=\delta_{\mu\mu'}\frac{d}{dR}+P_{\mu\mu'}. \tag{13}$$

In terms of ∂ and the adiabatic functions f_μ and g_μ Eq. (7) becomes

$$-\sum_{\mu'}\partial^2_{\mu\mu'}F_{\mu'\mu_0}=\left[\left(-\frac{d^2f_\mu}{dR^2}\right)a_{\mu\mu_0}+\left(-\frac{d^2g_\mu}{dR^2}\right)b_{\mu\mu_0}\right], \tag{14}$$

through the definition of f_μ and g_μ as solutions to the *uncoupled* equations. Splitting F into a and b in Eq. (9) has doubled the number of unknown functions to be determined, allowing us to impose any convenient relation between them. Following Babamov, we use this freedom to "factor" one ∂ from Eq. (14), requiring ∂ to act only on the adiabatic portion of the solution:

$$\sum_{\mu'}\partial_{\mu\mu'}F_{\mu'\mu_0}=\frac{df_\mu}{dR}a_{\mu\mu_0}+\frac{dg_\mu}{dR}b_{\mu\mu_0}. \tag{15}$$

Comparison of Eq. (15) with the explicit form of $\sum_{\mu'}\partial_{\mu\mu'}F_{\mu'\mu_0}$ identifies the relation between a and b:

$$f_\mu\frac{da_{\mu\mu_0}}{dR}+g_\mu\frac{db_{\mu\mu_0}}{dR} =-\sum_{\mu'}\left(P_{\mu\mu'}f_{\mu'}a_{\mu'\mu_0}+P_{\mu\mu'}g_{\mu'}b_{\mu'\mu_0}\right). \tag{16}$$

A second application of ∂ to (15) gives a completely analogous relation, with f and g replaced by their derivatives. Combining these two relations and the normalization condition $f_\mu dg_\mu/dR-g_\mu df_\mu/dR=\pi/2$, we extract the system of equations for a and b:

$$\begin{aligned}\frac{da_{\mu\mu_0}}{dR}&=\sum_{\mu'}\left(L^{(aa)}_{\mu\mu'}a_{\mu'\mu_0}+L^{(ab)}_{\mu\mu'}b_{\mu'\mu_0}\right),\\ \frac{db_{\mu\mu_0}}{dR}&=\sum_{\mu'}\left(L^{(ba)}_{\mu\mu'}a_{\mu'\mu_0}+L^{(bb)}_{\mu\mu'}b_{\mu'\mu_0}\right),\end{aligned} \tag{17a}$$

where

$$\begin{aligned}L^{(aa)}_{\mu\mu'}&=-\frac{\pi}{2}P_{\mu\mu'}W(g_\mu,f_{\mu'}),\\ L^{(ab)}_{\mu\mu'}&=-\frac{\pi}{2}P_{\mu\mu'}W(g_\mu,g_{\mu'}),\\ L^{(ba)}_{\mu\mu'}&=\frac{\pi}{2}P_{\mu\mu'}W(f_\mu,f_{\mu'}),\\ L^{(bb)}_{\mu\mu'}&=\frac{\pi}{2}P_{\mu\mu'}W(f_\mu,g_{\mu'}),\end{aligned} \tag{17b}$$

and $W(f,g)=fdg/dR-gdf/dR$ is the Wronskian of f and g. The interaction matrix appears thus "dressed" by the basis functions, as in Eq. (14) of Ref. [22], with the concept of dressing extended to include dressing by the derivatives of the basis functions.

The equation for the K matrix follows now just as in Eq. (18) of Ref. [22], by differentiating (11) and substituting the derivatives (17):

$$\frac{dK_{\mu\mu'}}{dR}=L^{(ba)}_{\mu\mu'}+\sum_{\mu''}\left(L^{(bb)}_{\mu\mu''}K_{\mu''\mu'}-K_{\mu\mu''}L^{(aa)}_{\mu''\mu'}\right) -\sum_{\mu''\mu'''}K_{\mu\mu''}L^{(ab)}_{\mu''\mu'''}K_{\mu'''\mu'}. \tag{18}$$

The initial condition for K follows from that for b, namely, $K(0)=0$. This condition, along with the symmetries of the L matrices,

$$L^{(ba)}_{\mu\mu'}=L^{(ba)}_{\mu'\mu},\ L^{(ab)}_{\mu\mu'}=L^{(ab)}_{\mu'\mu},\ L^{(aa)}_{\mu\mu'}=-L^{(bb)}_{\mu'\mu}, \tag{19}$$

ensure the symmetry of $K(R)$ for all R.

C. Elimination of closed channels

The K matrix begins the job of mixing the adiabatic functions but cannot complete it without reference to boundary conditions at $R\to\infty$. Specifically, contributions to the wave function from energetically closed channels must vanish at infinity, requiring a particular superposition of the Ψ_{μ_0}'s of Eq. (6). To achieve this superposition, we express the wave function in terms of the R-dependent coefficients $A_p(R)$ of eigenchannel functions $\psi_p(R,\omega)$,

$$\Psi=\sum_p A_p(R)\psi_p, \tag{20}$$

$$\psi_p=\sum_\mu\langle p|\mu\rangle\alpha_\mu\sin(\phi_\mu+\delta_p)\,\Phi_\mu. \tag{21}$$

We now treat each R separately as a matching radius for the MQDT procedure [26,31]. (A similar application of MQDT to mixing adiabatic functions was performed recently by Sadeghpour [32], with a *fixed* matching radius.) For a given radius, $\langle p|\mu(R)\rangle$ and $\delta_p(R)$ represent the channel coupling at smaller radii. Thereafter, MQDT considers the channels as independent, evolving only through their Milne phases $\phi_\mu(R)$. Within this framework, the condition for a closed channel μ to vanish at infinity involves the *asymptotic* Milne phase $\tilde{\phi}_\mu=\lim_{R\to\infty}\phi_\mu(R)$ through the condition

$$\sum_p A_p(R)\langle p(R)|\mu\rangle\sin[\tilde{\phi}_\mu+\delta_p(R)]=0\ . \tag{22}$$

This elimination of closed channels rearranges the open ones into new eigenchannels ρ, each with a common eigenphase shift $\pi\tau_\rho$. These τ's are defined for open μ by

$$\begin{aligned}\sum_p A_p\langle p|\mu\rangle\cos\delta_p&=T_{\mu\rho}\cos(\pi\tau_\rho),\\ \sum_p A_p\langle p|\mu\rangle\sin\delta_p&=T_{\mu\rho}\sin(\pi\tau_\rho).\end{aligned} \tag{23}$$

The quantities A_p and τ then follow from a generalized eigenvalue problem [31]

$$\Gamma A=\tan(\pi\tau)\,\Lambda A, \tag{24a}$$

where

$$\Gamma_{\mu p}=\begin{cases}\langle p|\mu\rangle\sin\delta_p & \text{if } \mu \text{ open}\\ \langle p|\mu\rangle\sin(\tilde{\phi}_\mu+\delta_p) & \text{if } \mu \text{ closed},\end{cases} \tag{24b}$$

$$\Lambda_{\mu p}=\begin{cases}\langle p|\mu\rangle\cos\delta_p & \text{if } \mu \text{ open}\\ 0 & \text{if } \mu \text{ closed}.\end{cases} \tag{24c}$$

We normalize the eigenvectors $T_{\mu\rho}$ to $\sum_\mu |T_{\mu\rho}|^2 = 1$, with the sum over *open* channels only, to preserve the energy normalization in the limit of large R.

The procedure outlined above amounts, at each R, to a *full* integration of the wave function up to R, then an *adiabatic* integration beyond R. Accordingly, the eigenquantum defects $\tau_\rho(R)$ vary most rapidly with R in regions of strongest channel coupling. By the same token, as R grows beyond the range of channel coupling, each τ_ρ settles into its asymptotic value $\tilde{\tau}_\rho = \lim_{R\to\infty} \tau_\rho(R)$. For open channels μ, ϕ_μ at large R represents the adiabatic phase of the escaping electron, and $\pi\tilde{\tau}_\rho$ is the phase shift contributed by interactions at short range. The asymptotic eigenquantum defect $\tilde{\tau}_\rho$ is a sensitive function of the total energy E, rising by unity when E passes through a resonance.

Mixing of the hyperspherical harmonics $u_{l_1 l_2 n_r}$ thus proceeds in three steps, each with its own notation: (1) The u's are combined into adiabatic functions Φ_μ; (2) diabatic corrections produce an evolving reaction matrix $K_{\mu\mu'}$, whose eigenvalues are indexed by p; (3) finally, MQDT mixes the different p's into the eigenchannels ρ, characterized by eigenquantum defects τ_ρ.

III. RESULTS

We proceed now to illustrate the behavior of eigenchannel functions through their R-dependent parameters τ_ρ and $T_{\mu\rho}$. In this pilot study we restrict our attention to the $^1S^e$ symmetry of He, and to resonances loosely classified by their independent-electron quantum numbers as $2sns$, in the energy range 57 eV $\leq E \leq$ 65 eV above the ground state. More precisely, the resonances considered correspond in the Herrick-Lin classification scheme [12] to levels indexed by ${}_n(K,T)^A_N = {}_n(+1,0)^+_2$. In this scheme, $K > 0$ ($K < 0$) denotes localization near $\theta_{12} = \pi$ ($\theta_{12} = 0$), while $A = +$ ($-$) indicates positive (negative) reflection symmetry of the functions Φ_μ across $\alpha = \pi/4$. N indexes the ionization limit of the channel, and n a level within that channel. Wave functions in this channel have predominantly an s^2 character, but allow an admixture of p^2 as well. The other adiabatic channel converging to the $N = 2$ threshold, namely, ${}_2(-1,0)^+_2$, will be ignored in this work.

A. The adiabatic channels

Figure 1 shows, for purposes of orientation, the three lowest adiabatic potential curves as calculated from Eq. (5). The channels, labeled in ascending order as $\mu = 1,2,3$, correspond to $(K,T)^A_N = (0,0)^+_1, (+1,0)^+_2, (-1,0)^+_2$, respectively. The dotted line in Fig. 1 represents $E = 57.8$ eV, roughly the energy of the ${}_2(+1,0)^+_2$ resonance. As the figure shows, the $\mu = 1$ channel is energetically open at this energy, while the $\mu = 2$ channel is energetically closed. The $\mu = 3$ channel is "strongly closed," i.e., the channel's kinetic energy $E - V_{\mu=3}(R)$ never becomes positive. For the remainder of this work, we will ignore this and all other strongly closed channels.

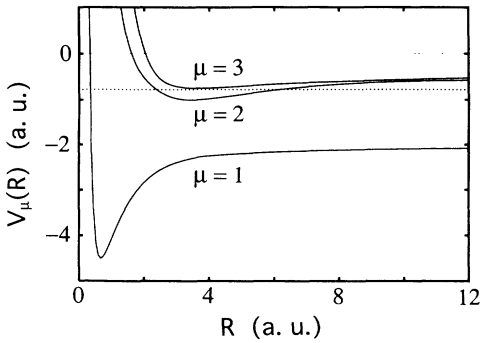

FIG. 1. The three lowest adiabatic potential curves $V_\mu(R)$. The dashed line indicates the energy of the double-ionization threshold, while the dotted line denotes 57.8 eV above the ground state, the approximate peak energy of the ${}_2(+1,0)^+_2$ resonance.

The relevant structure of the adiabatic functions $f_\mu(R)\Phi_\mu(R;\omega)$ is displayed in Fig. 2 at an energy $E =$ 57.8 eV. As we are interested primarily in radial correlations, we plot these functions in the r_1-r_2 plane, fixing $\theta_{12} = \pi$. The $\mu = 1$ channel, shown in Fig. 2(a), straddles the ridge at small R, owing to the dominance of centrifugal forces there. Beyond about $R \simeq 2$ a.u. the ridge lies at such a high potential that the system instead seeks out the valleys. In this case one electron remains near the nucleus while the other escapes with a radial coordinate $\sim R$. The nodal pattern beyond $R \simeq 3$ a.u. represents the escape of one or the other electron to infinity. (As an aside, we note that the valley localization described here requires an increasingly large number of

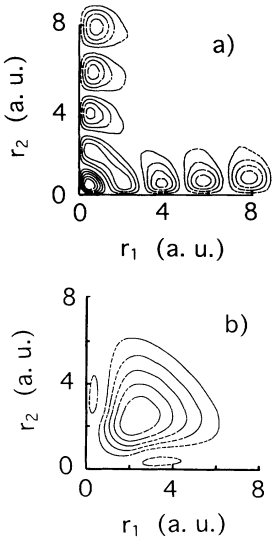

FIG. 2. Contour plots of adiabatic channel functions in the r_1-r_2 plane: (a) $\mu = 1$, showing the escape of this channel into potential valleys at large R; (b) $\mu = 2$, showing ridge localization near $R \simeq$ 3–4 a.u. The behavior of this function at larger R, where it also falls into the potential valleys, is not shown here.

hyperspherical harmonics with increasing values of n_r. The adiabatic approximation accounts instead for the localization through a *single* channel.)

The $\mu = 2$ adiabatic channel shown in Fig. 2(b) displays a different correlation pattern in the same radial range. This channel, *constrained* at each R to be *orthogonal* to $\mu = 1$, remains on the ridge up to a larger R. It begins to localize in the valley at $R \simeq 8$ a.u., behavior excluded from the figure. The channel function's main feature consists of a single radial antinode between the classical turning points, 2 a.u. $\leq R \leq 6$ a.u. Beyond this radius f_μ diverges unless the total energy belongs to a discrete set of eigenvalues. This is the basis of the zeroth-order adiabatic approximation to the doubly excited states [11]. Coupling to $\mu = 1$ allows instead the total wave function to be finite at large R for any value of E. In addition to the large ridge localization, this channel exhibits a small amplitude in the valley near $R \simeq 3-4$ a.u.

Putting these two pictures together, we see that the channels interact mainly in two regions of configuration space: (1) $R \simeq 2-3$ a.u., where the channels meet on the ridge; and (2) $R \geq 3-4$ a.u., $\alpha \simeq 0$ (or $\alpha \simeq \pi/2$), where the closed channel interferes with the escaping open channel. We expect the importance of the second region to be secondary in determining the resonance, because the $\mu = 2$ channel has much lower amplitude there than on the ridge.

B. The $_2(+1,0)_2^+$ resonance

The first step in studying the $_2(+1,0)_2^+$ resonance is to identify it. Only one eigenquantum defect τ, corresponding to the single open channel, exists near the resonance energy. The variation of τ with R is shown in Fig. 3(a) for several, equally spaced, energies. As anticipated, τ varies within an "interaction region," 3 a.u. $\leq R \leq 8$ a.u., then settles into its asymptotic value $\tilde{\tau}$. The sudden change in the profile of τ as the energy varies signals the resonance near these energies. Figure 3(b) shows the energy derivative of the long-range eigenquantum defect, $d\tilde{\tau}/dE$, which represents the "time delay" in the scattering of electrons by ground state He ions [33]. That is, $d\tilde{\tau}/dE$ represents the amount of time an incident wave packet is delayed at short range by its interaction with the closed channel. The peak position and full width at half maximum FWHM of the resonance, determined from $d\tilde{\tau}/dE$, are $E_0 = 57.8$ eV and $\Gamma = 0.10$ eV, in good agreement with typical measured values of $E_0 = 57.8$ eV and $\Gamma = 0.14$ eV [34].

The negative value of $\tau(R)$ below resonance can be understood as follows: The $_2(+1,0)_2^+$ resonance arises from the coupling of the open $\mu = 1$ channel to the lowest bound state of the potential $V_2(R)$. However, due to the repulsion of levels between $\mu = 1$ and $\mu = 2$, the actual resonance energy is *greater* than the bound state energy. The $\mu = 2$ component of the resonant wave function is thus represented by an adiabatic function $f_2\Phi_2$ containing a radial node, although the resonance itself has no such node. Accordingly, the eigenphase shift $\pi\tau(R)$ evolves toward a value near $-\pi$, removing the artificial

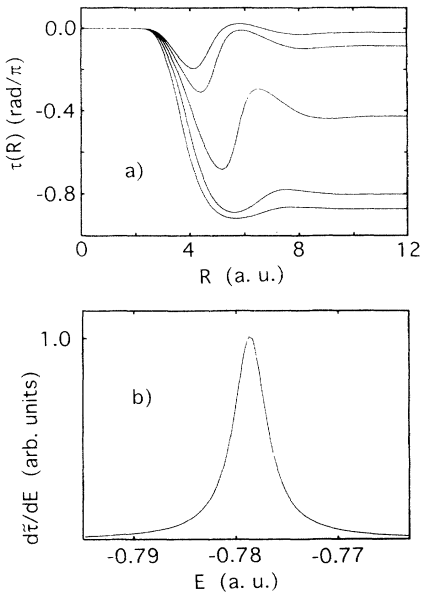

FIG. 3. (a) Eigenquantum defect $\tau(R)$ near the $_2(+1,0)_2^+$ resonance, showing the general profile of τ and its sudden rise at resonance. The energies shown are $E_0 - 2\Gamma$, $E_0 - \Gamma$, E_0, $E_0+\Gamma$, $E_0+2\Gamma$; (b) energy derivative $d\tilde{\tau}/dE$ of the asymptotic eigenquantum defect $\tilde{\tau}$, which determines the peak position and width of the resonance as E =57.8 eV and Γ =0.10 eV.

node. As the energy rises through the resonance, the resonant wave function acquires a real radial node, as evidenced by the rise of $\tilde{\tau}$. Above resonance, $f_2\Phi_2$ represents the state adequately; thus $\tau(R)$ remains near zero.

The profile of $\tau(R)$ serves as a record of the channel interactions. In accordance with the remarks of Sec. II A, we consider two regions of interaction: (1) $R \leq 4$ a.u. on the ridge, (2) $R \geq 4$ a.u. in the valley.

(1) First, for $R \leq 2$ a.u., $\mu = 2$ remains suppressed by its generalized centrifugal barrier, so that the channel interaction is minimal, and $\tau = 0$. Next, τ falls steeply with increasing R, indicating strong channel interactions. Figure 4 illustrates the effect of these interactions by showing the eigenchannel function Ψ *on the ridge* as a function of R alone. The dashed and dotted lines indicate the individual amplitudes in the $\mu = 1$ and $\mu = 2$ channels, respectively. At $R \simeq 2$ a.u. the amplitude shifts smoothly,

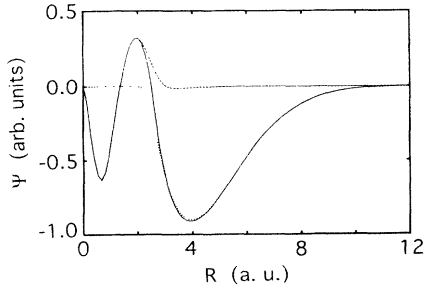

FIG. 4. *Solid curve*: the $_2(+1,0)_2^+$ resonant wave function as a function of R for $\alpha = \pi/4$, $\theta_{12} = \pi$. *Dashed curve*: Contribution by the $\mu = 1$ channel. *Dotted curve*: Contribution by the $\mu = 2$ channel.

and *in phase*, from one channel to the other. The combined result, shown as a solid line, represents a standing wave extending from $R = 0$ to the outer turning point.

This connection of channels at short range is the mechanism whereby $\mu = 2$ gains or sheds the amplitude necessary to remain convergent at large R. The resonance occurs when amplitude entering $\mu = 2$ meets reflected amplitude leaving $\mu = 2$ with the correct relative phase. As the total energy increases, the wavelength in $\mu = 1$ decreases, while the range of R accessible to $\mu = 2$ increases. Roughly speaking, resonance occurs when these two lengths coincide.

The dominant role of short-range interactions in determining the resonance is apparent in the profile of τ [Fig. 3(a)]. The PA method calculates, at each R, the eigenquantum defect pertaining to channel interactions at smaller R, regarding the channels as independent beyond that R. Even at $R \simeq 4$ a.u. τ climbs by nearly unity as the energy passes through resonance. Thus, while large-R interactions determine some details, they do not account for the resonance itself.

(2) For $R \geq 4$ a.u. the small valley portion of $\mu = 2$ interferes with $\mu = 1$, alternatively helping or hindering its motion. In particular, in the range $R \simeq 5$–6 a.u., $\mu = 2$ meets its outer turning point and reflects from it. Total reflection occurs only on the ridge, whereas amplitude in the valley leaks out, giving an additional outward boost to $\mu = 1$. This boost manifests itself as an effective repulsive potential, or equivalently a rising τ, whose effect is most prominent at the resonant energy. Other, less significant, features of τ arise from interferences of $\mu = 1$ with the long decaying tail of $\mu = 2$.

C. The ${}_n(+1,0)_2^+$ resonances

The ${}_2(+1,0)_2^+$ resonance represents the coupling with the continuum of the lowest adiabatic bound state in the $\mu = 2$ channel. Higher bound states in this channel also correspond to higher resonances, of the type ${}_n(+1,0)_2^+$. In the relevant energy range, 58 eV $\leq E \leq$ 65 eV, the $\mu = 3$ channel referred to above becomes weakly closed, as opposed to strongly closed. However, as this channel contributes mostly to resonances with $K = -1$, localized in a different region of configuration space, we continue to neglect its influence.

The eigenquantum defect τ is pictured in Fig. 5 for several energies near the ${}_3(+1,0)_2^+$ resonance. These energies lie above the second bound state of $V_2(R)$. As was the case near the ${}_2(+1,0)_2^+$ resonance, the adiabatic function $f_2\Phi_2$ contains an additional, unphysical radial node, requiring that $\tau(R)$ be "reset" to negative values. The profile of τ is qualitatively the same as for the ${}_2(+1,0)_2^+$ resonance, but extends to the larger R appropriate to the higher energy. In particular, the negative slope of τ in the region 2 a.u. $\leq R \leq 4$ a.u. indicates the same short-range channel coupling as above. The peak position and width of the ${}_3(+1,0)_2^+$ resonance, determined from $d\bar{\tau}/dE$, are $E_0 = 63.5$ eV and $\Gamma = 0.071$ eV, as compared to measured values of $E_0 = 62.9$ eV and $\Gamma = 0.045$ eV [34].

At higher excitations, $\mu = 2$ lies further in the valley,

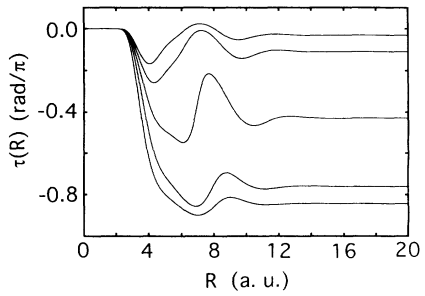

FIG. 5. Eigenquantum defect $\tau(R)$ near the ${}_3(+1,0)_2^+$ resonance. Note its similarity to Fig. 3(a).

but not so far as $\mu = 1$, implying minimal interaction at large R. We thus anticipate that the entire ${}_n(+1,0)_2^+$ series is excited in the same way, by the exchange of channel amplitude near $R \simeq 2$ a.u. This view emerges only when we consider the evolution of the doubly excited state from the origin outward. To calculate the higher ${}_n(+1,0)_2^+$ resonances, we exploit the slow variation of the short-range K matrix with energy within a core radius $R \leq 10$ a.u. Then, standard MQDT, using independent-electron Coulomb wave functions outside the core, identifies the resonances. Results for some of these resonances are presented in Table I.

IV. DISCUSSION

In this work, we have focused on a particular series of doubly excited resonances in He($^1S^e$), to show how the PA method, combined with MQDT, opens a window into the dynamics, previously hidden within calculations. Extension of the results reported here will require the following improvements.

Numerical accuracy. All adiabatic potentials and coupling matrices have been calculated without regard to optimum accuracy, but adequately for our illustrative purposes. However, as we proceed to higher energies, we will require greater accuracy, both to ensure convergence at large R and to deal adequately with the increasing number of channels. Recent work [32,36,37] has significantly improved the ability to calculate accurate adiabatic functions.

Additional resonances and symmetries. Each bound state of each adiabatic potential (above $\mu = 1$) pro-

TABLE I. Comparison of this work's approximate resonance peaks with the accurate results of Ref. [35], referred to the ground state 79.0 eV below the double-ionization threshold.

Resonance ${}_n(+1,0)_2^+$	This work E_0 (eV)	Ref. [35] E_0 (eV)
$n = 2$	57.8	57.8
$n = 3$	63.5	62.9
$n = 4$	64.4	64.2
$n = 5$	64.7	64.7
$n = 6$	65.1	64.9

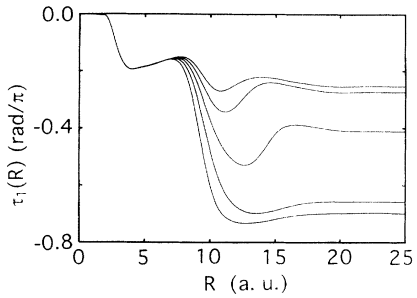

FIG. 6. One of the three eigenquantum defects near the ${}_3(+2,0)_3^+$ resonance, showing the connection between ${}_2(+1,0)_2^+$ and ${}_3(+2,0)_3^+$ states. See text for details.

duces an autoionizing resonance like the ones reported here. Even off resonance, the channels interfere with each other, in ways that remain to be explored by the PA method. In addition, future applications will extend to values of the total angular momentum beyond $L = 0$.

Influence of strongly closed channels. We have ignored strongly closed channels here without hurting our general conclusions. However, in calculating cross sections at energies below the $N = 2$ threshold, Sadeghpour [32] needed to include all the adiabatic channels converging to the $N = 3$ threshold. To do the same, we must fit the strongly closed channels into the PA formalism.

Multiple open channels. Above the $N = 2$ threshold, the number of open channels increases, diverging at the double-ionization threshold. In this case, multiple eigenquantum defects τ_ρ will emerge, complicating the interpretation of the dynamics. The closed channels produce resonances, identified by a rise in the *sum* $\sum_\rho \tau_\rho$ by unity. In Fig. 6 we show a single τ_ρ for the "$3s^2$" resonance, near its resonance energy, $E_0 = 69.5$ eV. Near $R \simeq 3$ a.u., τ_ρ exhibits a negative slope, a remnant of the coupling between $\mu = 1$ and $\mu = 2$ discussed above. Near $R \simeq 7$ a. u. τ_ρ again has a negative slope, this time signifying the coupling between the $\mu = 2$ channel (now open) and the resonant ridge channel, classified as $(K,T)_N^A = (2,0)_3^+$. This τ_ρ thus establishes a connection between successive ridge resonances, absent in the adiabatic approximation. As the energy rises to the double-ionization threshold, τ_ρ connects each "Ns^2" state to the next, "$(N+1)s^2$" state, uniting the entire double Rydberg series.

Note added. J. Light has brought to my attention similar work by M. H. Alexander [38], who studies the evolution of flux transfer between adiabatic channels in molecular physics. I am indebted to Dr. Light for this information.

ACKNOWLEDGMENTS

This work was supported by the National Science Foundation Grant No. PHY 90-19966. I wish to thank U. Fano, E. Sidky, and J. Macek for fruitful discussions. I also thank F. Robicheaux for a critical reading of an earlier draft.

[1] G. Wannier, Phys. Rev. **90**, 817 (1953).
[2] A. R. P. Rau, Phys. Rev. A **4**, 207 (1971).
[3] R. Peterkop, J. Phys. B **4**, 513 (1971).
[4] A. R. P. Rau, J. Phys. B **16**, L699 (1983).
[5] M. Aymar, J. Phys. B **22**, 2359 (1989).
[6] Y. Komninos and C. A. Nicolaides, J. Phys. B **19**, 1701 (1986); M. Chrysos, Y. Komninos, Th. Mercouris, and C. A. Nicolaides, Phys. Rev. A **42**, 2634 (1990).
[7] Y. K. Ho, Phys. Rev. A **35**, 2035 (1987); **41**, 1492 (1990).
[8] P. F. O'Mahoney and C. H. Greene, Phys. Rev. A **31**, 250 (1985).
[9] J. Callaway, Phys. Rev. A **37**, 3692 (1988).
[10] J. Shertzer and F. S. Levin, Phys. Rev. A **43**, 2531 (1991); J. Botero and J. Shertzer, *ibid.* **46**, 1155 (1992).
[11] J. Macek, J. Phys. B **1**, 831 (1968).
[12] C. D. Lin, Adv. At. Mol. Phys. **22**, 77 (1986).
[13] C. D. Lin, Phys. Rev. A **10**, 1986 (1974).
[14] J. M. Feagin and J. S. Briggs, Phys. Rev. A **37**, 4599 (1988); J. M. Rost and J. S. Briggs, J. Phys. B **24**, 4293 (1991).
[15] D. R. Herrick, Phys. Rev. A **12**, 413 (1975).
[16] H. Fukada, N. Koyama, and M. Matsuzawa, J. Phys. B **20**, 2959 (1987); N. Koyama, A. Takofuji, and M. Matsuzawa, *ibid.* **22**, 553 (1989).
[17] J. M. Rost and J. S. Briggs, J. Phys. B **21**, L233 (1988); **22**, 3587 (1989).
[18] H. R. Sadeghpour and C. H. Greene, Phys. Rev. Lett. **65**, 313 (1990).
[19] J. Tang, S. Watanabe, and M. Matsuzawa, Phys. Rev. A **46**, 2437 (1992).
[20] S. Cvejanović and F. H. Read, J. Phys. B **7**, 1841 (1974).
[21] S. J. Buckman, P. Hammond, F. H. Read, and G. C. King, J. Phys. B **16**, 4039 (1983).
[22] U. Fano and E. Y. Sidky, Phys. Rev. A **45**, 4776 (1992); E. Y. Sidky, *ibid.* **47**, 2812 (1993).
[23] F. T. Smith, Phys. Rev. **120**, 1058 (1960).
[24] U. Fano, Phys. Rev. A **24**, 2402 (1981).
[25] J. L. Bohn (unpublished).
[26] M. J. Seaton, Rep. Prog. Phys. **46**, 167 (1983).
[27] Y. F. Smirnov and K. V. Shitikova, Fiz. Elem. Chastits At. Yadra **8**, 847 (1977) [Sov. J. Part. Nucl. **8**, 344 (1977)]; J. M. Feagin, J. Macek, and A. F. Starace, Phys. Rev. A **32**, 3219 (1985).
[28] W. E. Milne, Phys. Rev. **35**, 863 (1930); F. Robicheaux, U. Fano, M. Cavagnero, and D. A. Harmin, Phys. Rev. A **35**, 3619 (1987).
[29] C. Zemach, Nuovo Cimento **33**, 939 (1964); A. Degasperis, *ibid.* **34**, 1667 (1964); F. Calogero, *Variable Phase Approach to Potential Scattering* (Academic, New York, 1967), Chap. 19.
[30] V. K. Babamov, J. Chem. Phys. **69**, 3414 (1978).
[31] C. H. Greene and Ch. Jungen, Adv. At. Mol. Phys. **21**, 51 (1985).
[32] H. R. Sadeghpour, Phys. Rev. A **43**, 5821 (1991); H. R. Sadeghpour, J. Phys. B **25**, L29 (1992).
[33] F. T. Smith, Phys. Rev. **118**, 349 (1960).

[34] P. J. Hicks and J. Comer, J. Phys. B **8**, 1866 (1975), and references therein.
[35] D. H. Oza, Phys. Rev. A **33**, 824 (1986).
[36] J. Q. Sun and C. D. Lin, Phys. Rev. A **46**, 5489 (1992)
[37] H. T. Coelho, J. J. DeGroote, and J. E. Hornos, Phys. Rev. A **46**, 5443 (1992).
[38] M. H. Alexander, J. Chem. Phys. **95**, 8931 (1991); D. E. Manolopoulos and M. H. Alexander, J. Chem. Phys. **97**, 2527 (1992).